point and ~400 cm^{-1} above the ground level of the ^5T manifold.

The magnitude of the interaction energy is ~100 cm^{-1} for both d^5 and d^6 systems,[31-33] implying that intersystem crossing is not highly forbidden for either d^5 or d^6 spin equilibria. This is certainly consistent with the lower limits for κ of 10^{-2}–10^{-3} obtained for $[Fe(acac_2trien)]^+$, $[Fe(Sal_2trien)]^+$, and $Fe(paptH)_2]^{2+}$. However, the smaller minimum value for κ of $10^{-4.2}$ found for $[Fe(HB(pz)_3)_2]$ may indicate differences in the extent of mixing at the crossover point among different complexes.[3]

In summary, ultrasonic absorption measurements for aqueous solutions of $[Fe(acac_2trien)]^+$ reveal single ultrasonic relaxation processes with the relaxation time of 2.11 ± 0.04 ns at 25 °C being concentration independent over the range 0.02–0.10 M. This is similar to the results obtained previously for $[Fe(Sal_2trien)]^+$, for which a relaxation time of 5.33 ± 0.05 ns was observed at 25 °C in distilled water.[4] These values for the relaxation times are consistent with the results of our laser temperature-jump experiments for aqueous and methanol solutions of the complexes, which also reveal no apparent concentration dependence of the relaxation times. Independent estimates for the volume differences, ΔV°, obtained from the pressure dependence of the spectra are consistent with the values obtained from the ultrasonic relaxation amplitudes. The temperature dependences of the ultrasonic relaxation amplitudes are also consistent with the temperature dependences of the spin equilibria as determined from magnetic susceptibility measurements. The ultrasonic relaxations are therefore ascribed to unimolecular isomerizations of the iron(III) complexes between two states of different spin multiplicity. With use of the ΔV° values obtained from the ultrasonic relaxation amplitudes, the average metal–ligand bond length differences between the two spin states are calculated to be 0.11 and 0.13 Å for $[Fe(acac_2trien)]^+$ and $[Fe(Sal_2trien)]^+$, respectively, in excellent agreement with the X-ray structural data for these complexes.[20]

The accuracy of the ultrasonic relaxation technique permits the evaluation of the activation parameters for these formally spin-forbidden $\Delta S = 2$ intersystem-crossing processes, revealing significant activation enthalpies in *both* directions. With use of absolute rate theory, the minimum value of the transmission coefficient is $10^{-2.5}$ for $[Fe(acac_2trien)]^+$ and $10^{-3.0}$ for $[Fe(Sal_2trien)]^+$. Thus, both thermodynamic barriers and electronic factors contribute substantially to the free-energy barriers for intersystem crossing in these iron(III) complexes. Therefore, the intersystem-crossing process in these systems can be described as a nonadiabatic, internal electron transfer between two distinct electronic isomers possessing different nuclear configurations, with the average metal–ligand bond length difference being 0.11–0.13 Å. Finally, it should be noted that unimolecular excited-state decay processes can compete with intersystem-crossing processes, so that κ values of ~10^{-2} will be important in determining the observed quantum yields of such processes.

Acknowledgment. The work at the University of Sydney was sponsored in part by the Australian Research Grants Committee and in part by the Sydney County Council. Acknowledgement if also made to the donors of The Petroleum Research Fund, administered by the American Chemical Society, for partial support of this work. The work at the University of Rochester was sponsored by NIH under Grants GM 22939-04 and 5T32GM07230. D.H.T. is an Alfred P. Sloan Fellow. We thank Dr. G. A. Lawrance for assistance with the high-pressure measurements at the University of Melbourne.

Supplementary Material Available: Tables II, III, and IV of the solution magnetic susceptibility data and Tables VI, VII, VIII, and IX of variable temperature/pressure spectral data (7 pages). Ordering information is given on any current masthead page.

Dynamic Properties of Phosphinehydridorhodium(I) Complexes and the Structure of Tris(triisopropylphosphine)hydridorhodium(I), $RhH(P(i\text{-}Pr)_3)_3$

T. Yoshida,[1a] David L. Thorn,[1b] T. Okano,[1a] Sei Otsuka,[1a] and James A. Ibers*[1b]

Contribution from the Department of Chemistry, Faculty of Engineering Science, Osaka University, Toyonaka, Osaka, Japan 560, and the Department of Chemistry, Northwestern University, Evanston, Illinois 60201. *Received March 12, 1980*

Abstract: The phosphinehydridorhodium(I) complexes $RhH(P(i\text{-}Pr)_3)_3$ (**1**) and $RhH(PEt_3)_3$ (**2**) undergo an intramolecular site exchange process similar to that of $RhH(PPh_3)_3$. In an attempt to understand this process, the crystal and molecular structure of tris(triisopropylphosphine)hydridorhodium(I), $RhH(P(i\text{-}Pr)_3)_3$ (**1**), has been determined at −150 °C. The complex crystallizes as yellow needles with two formula units in the triclinic space group C_i^1-$P\bar{1}$ in a cell of dimensions a = 11.615 (5) Å, b = 16.958 (8) Å, c = 8.680 (6) Å, α = 103.44 (2)°, β = 103.53 (2)°, γ = 82.98 (2)°, V = 1612 Å^3. The final conventional and weighted agreement indices on F_0 for 7082 reflections with $F_0^2 > 3\sigma(F_0^2)$ are 0.025 and 0.029, respectively. The molecule exhibits strictly planar coordination about the rhodium atom but the steric bulk of the triisopropylphosphine ligands has caused some unusual angular distortions about the rhodium and phosphorus atoms. The H–Rh–P(cis) angle is 70.7 (14)° (av), the smallest reported for planar structures. The Rh–P–C angles, usually in the range 111–117° in rhodium triisopropylphosphine complexes, span the range 109.28 (6) to 126.38 (6)° in the present complex. The Rh–H distance is 1.58 (2) Å, Rh–P (trans to H) is 2.330 (1) Å, and Rh–P (cis to H) are 2.291 (1) and 2.297 (1) Å. The difference in stereochemical rigidity of $RhH(PR_3)_3$ may be ascribed primarily to the steric requirements of the phosphine ligands. The tetrakisphosphine complex $RhH(PEt_3)_4$ (**3**) exists in equilibrium with **2** and PEt_3 and also is fluxional.

Introduction

We have recently studied the unusual coordination numbers and geometries imposed upon rhodium complexes by bulky phosphine ligands.[2-7] In earlier papers we have discussed the formation and properties of hydridodinitrogen rhodium bis(trialkyl)phosphine complexes,[2,5] and their tendency to lose the di-

---

(1) (a) Osaka University; (b) Northwestern University.

(2) Hoffman, P. R.; Yoshida, T.; Okano, T.; Otsuka, S.; Ibers, J. A. *Inorg. Chem.*, **1976**, *15*, 2462–2466.

(3) Yoshida, T.; Okano, T.; Otsuka, S. *J. Chem. Soc., Chem. Commun.*, **1978**, 855–856.

0002-7863/80/1502-6451$01.00/0

nitrogen ligand to form μ-dinitrogen dimers or nitrogen-free monomers or dimers.[2,5] These chloride-free, phosphine hydridorhodium complexes constitute part of a family of strong nucleophilic Rh(I) compounds capable of undergoing various substitution and addition reactions. For example, $(RhHL_2)_2(\mu\text{-}N_2)$ and $RhHL_3$ (L = $P(i\text{-}Pr)_3$) have been found to be active catalysts for H–D exchange reactions,[8] the hydrogenation of nitriles,[9] and the water–gas shift reaction.[4,10]

The tris(phosphine)hydridorhodium(I) compounds $RhH(P(i\text{-}Pr)_3)_3$ (**1**) and $RhH(PEt_3)_3$ (**2**) are of interest as members of this family of catalysts, and also because they exhibit fluxional behavior on the ^{31}P NMR time scale. A square-planar $\rightleftharpoons$ pseudotetrahedral interconversion has been suggested as a mechanism for intramolecular ligand site exchange in $RhH(PPh_3)_3$.[11] We thought that an X-ray structure determination of the sterically crowded compound $RhH(P(i\text{-}Pr)_3)_3$ (**1**) might reveal a significant distortion from nominal planar geometry which in turn could support a mechanism for the rearrangement process. In this paper we report the fluxional behaviors of the compounds $RhH(P(i\text{-}Pr)_3)_3$ (**1**), $RhH(PEt_3)_3$ (**2**), and $RhH(PEt_3)_4$ (**3**) and the low-temperature X-ray structure of **1**. Contrary to our expectations, the $RhH(P(i\text{-}Pr)_3)_3$ molecule has strictly planar coordination about the rhodium atom.

Experimental Section

^1H NMR, IR, and electronic spectra were recorded with a JEOL JNM-4H-100 spectrometer, a Hitachi Model 295 spectrometer, and a Hitachi EPS-3T spectrophotometer, respectively. $^{31}P\{^1H\}$ NMR spectra were measured with a JEOL JNH-FX100 spectrometer at 40.32 MHz, using 85% H_3PO_4 (21 °C) as an external reference. All reactions and manipulations were carried out under dinitrogen or argon atmospheres. Samples of $RhH(P(i\text{-}Pr)_3)_3$ (1) for $^{31}P\{^1H\}$ NMR measurements were prepared by the method reported previously.[5]

Preparation of Tetrakis(triethylphosphine)hydridorhodium(I), $RhH(PEt_3)_4$ (3). A mixture of $RhCl_3 \cdot 3H_2O$ (0.98 g, 4 mmol) and PEt_3 (1.45 g, 12 mmol) in THF (20 mL) was stirred at ambient temperature for 20 h. The mixture was dried in vacuo. The orange solid residue was suspended in THF (20 mL) containing PEt_3 (1.45 g, 12 mmol) and stirred at room temperature with 50 g of 1% sodium amalgam for 20 h. The solution was filtered and the filtrate was dried in vacuo to give dark green crystals. Recrystallization from cold *n*-pentane containing free PEt_3 (0.3 mL) gave pale yellow crystals (1.60 g, 70%), mp 45 °C (under Ar). IR: ν(H-Rh) 1997 cm^{-1}. Anal. Calcd for $C_{24}H_{61}P_4Rh$: C, 49.99; H, 10.66. Found: C, 48.83; H, 10.66.

Preparation of Tris(triethylphosphine)hydridorhodium(I), $RhH(PEt_3)_3$ (2). Crystals of tetrakis(triethylphosphine)hydridorhodium(I) (3, 0.24 g, 0.5 mmol) were heated to 60–65 °C in vacuo (10^{-3} mmHg) for 0.5 h to give a red oil in quantitative yield. IR: ν(H-Rh) 1928 cm^{-1}. Anal. Calcd for $C_{18}H_{46}P_3Rh$: C, 47.16; H, 10.16. Found: C, 46.92; H, 10.06.

X-ray Sample Preparation and Data Collection. The single crystals of $RhH(P(i\text{-}Pr)_3)_3$ (1) used for X-ray diffraction were serendipitously obtained during our attempt to prepare crystals of the previously described compound $[RhH(P(i\text{-}Pr)_3)_2]_2$.[3,5] The compound $[RhH(P(i\text{-}Pr)_3)_2]_2(\mu\text{-}N_2)$[5] (ca. 0.1 g) was dissolved in toluene, and argon was bubbled through the solution for 1 h. The solution was then concentrated under vacuum to ca. 1 mL and allowed to stand under argon for 1 month at −20 °C. Two kinds of crystals slowly grew in the solution: large, orange plates and smaller, yellow needles. One of the yellow needles was sealed in a capillary under argon and used for preliminary X-ray photographic examination. Weissenberg and precession photographs of this crystal revealed no symmetry, other than the trivial center of symmetry, and cell constants consistent only with a triclinic space group. The observed density of 1.17 (1) g/cm^3, measured by flotation in aqueous $ZnCl_2$, is in excellent agreement with the density 1.17 g/cm^3 calculated for two molecules of $RhH(P(i\text{-}Pr)_3)_3$ in the cell, and this formulation is confirmed by the completed structure.

Table I. Summary of Crystal Data and Intensity Collection for $RhH(P(i\text{-}Pr)_3)_3$ (1)

compd	$RhH(P(i\text{-}Pr)_3)_3$
formula	$C_{27}H_{64}P_3Rh$
temp	−150 °C[a]
formula wt	584.64 amu
space group	C_i^1-$P\bar{1}$
a	11.615(5) Å
b	16.958(8) Å
c	8.680(6) Å
α	103.44(2)°
β	103.53(2)°
γ	82.98(2)°
V	1612 $Å^3$
Z	2
density (calcd)	1.204 g/cm^3 (−150 °C)
density (obsd)	1.17(1) g/cm^3 (23 °C)
crystal shape and dimensions[b]	column, ends of form {001} (0.88), sides of forms {010} (0.19), {110} (0.17)
crystal vol	0.035 mm^3
radiation	Mo Kα (λ(Mo Kα_1) = 0.709 300 Å)
linear absorption coefficient	6.80 cm^{-1}
transmission factors	0.839–0.914, av 0.884
take-off angle	2.7°
scan method	continuous θ–2θ scan
scan speed	2.0° in 2θ/min
scan range	1.1° below Kα_1 peak to 1.0° above Kα_2 peak
2Θ limits	4.0–57.1°
background collection	10 s with rescan option[c]
final no. of variables	284
unique data used in final refinement[d]	8214
unique data, $F_o^2 > 3\sigma(F_o^2)$	7082
R (on F_o^2, all data)	0.041
R_w (on F_o^2, all data)	0.061
R (on F_o for $F_o^2 > 3\sigma(F_o^2)$)	0.025
R_w on F_o for ($F_o^2 > 3\sigma(F_o^2)$)	0.029
error in observation of unit weight	1.15 $electrons^2$

[a] See ref 13. [b] The perpendicular distance between the indicated face and its Friedel mate is given in millimeters in parentheses. [c] See ref 12. [d] This includes reflections with $F_o^2 < 0$.

For data collection this needle-shaped crystal was removed from its capillary and mounted on a four-circle, computer-controlled[12] Picker diffractometer. Throughout the data collection the crystal was continuously bathed in a stream of cold (−150 °C) nitrogen gas.[13] At this temperature the unit cell constants, derived from the setting angles of 17 hand-centered reflections[14] in the range 25° < 2θ(Mo Kα) < 29°, are a = 11.615 (5) Å, b = 16.958 (8) Å, c = 8.680 (6) Å, α = 103.44 (2)°, β = 103.53 (2)°, γ = 82.98 (2)°, V = 1612 $Å^3$. A Delaunay reduction did not reveal any hidden symmetry. A total of 8744 reflections (8214 unique) was measured for 2θ in the range 4–57.1°. Six strong reflections were remeasured every 100 reflections during the course of the data collection, and their intensities showed insignificant fluctuations or changes. Other parameters relevant to the data-collection process are listed in Table I.

Solution and Refinement of the Structure. Solution and refinement of the structure were carried out by procedures standard in this laboratory.[15] The positions of the rhodium and the three phosphorus atoms were easily

---

(4) Yoshida, T.; Thorn, D. L.; Okano, T.; Ibers, J. A.; Otsuka, S. *J. Am. Chem. Soc.*, **1979**, *101*, 4212–4220.

(5) Yoshida, T.; Okano, T.; Thorn, D. L.; Tulip, T. H.; Otsuka, S.; Ibers, J. A. *J. Organomet. Chem.* **1979**, *181*, 183–201.

(6) Yoshida, T.; Otsuka, S.; Matsumoto, M.; Nakatsu, K. *Inorg. Chim. Acta* **1978**, *29*, L257–L259.

(7) Thorn, D. L.; Tulip, T. H.; Ibers, J. A. *J. Chem. Soc., Dalton Trans.* **1979**, 2022–2025.

(8) Yoshida, T.; Okano, T.; Saito, K.; Otsuka, S. *Inorg. Chim. Acta*, **1980**, *44*, L135–L136.

(9) Yoshida, T.; Okano, T.; Otsuka, S. *J. Chem. Soc., Chem. Commun.* **1979**, 870–871.

(10) Yoshida, T.; Okano, T.; Otsuka, S., to be published.

(11) Strauss, S. H.; Diamond, S. E.; Mares, F.; Shriver, D. F. *Inorg. Chem.* **1978**, *17*, 3064–3068.

(12) The disk-oriented diffractometer control program is from Lenhert, P. G. *J. Appl. Crystallogr.* **1975**, *8*, 568–570.

(13) Huffman, J. C. Ph.D. Thesis, Indiana University, 1974.

(14) Corfield, P. W. R.; Doedens, R. J.; Ibers, J. A. *Inorg. Chem.* **1967**, *6*, 197–204.

(15) See, for example, Waters, J. M.; Ibers, J. A. *Inorg. Chem.* **1977**, *16*, 3273–3277.

Table II. Positional and Thermal Parameters for the Atoms of $RhH(P(i\text{-}Pr)_3)_3$

ATOM	X[A]	Y	Z	B11[B] OR B,Å^2	B22	B33	B12	B13	B23
RH	-0.195957(11)	0.241025(10)	0.149048(15)	18.96(10)	8.28(5)	28.79(18)	-1.79(4)	5.59(9)	1.35(6)
P(1)	-0.362662(37)	0.181031(25)	-0.008249(51)	22.66(30)	9.61(14)	38.15(58)	-3.31(16)	3.93(33)	2.95(23)
P(2)	-0.247670(36)	0.375703(25)	0.261164(50)	23.63(30)	8.99(14)	32.50(56)	-1.77(16)	7.65(32)	2.08(22)
P(3)	0.004974(37)	0.214131(26)	0.231296(51)	21.69(30)	10.89(14)	34.38(57)	-0.99(16)	6.36(32)	3.45(23)
C(11)	-0.40250(15)	0.09871(10)	0.07599(22)	30.7(13)	11.79(58)	60.7(25)	-6.72(69)	5.5(14)	6.44(97)
C(12)	-0.32967(16)	0.12306(11)	-0.20626(21)	34.0(13)	14.58(62)	44.8(24)	-5.85(73)	5.3(14)	0.59(98)
C)13)	-0.51314(15)	0.23522(11)	-0.06017(22)	27.0(13)	12.76(60)	67.5(26)	-1.12(69)	1.1(14)	5.5(10)
C(14)	-0.30481(18)	0.03038(11)	0.09327(26)	47.4(16)	13.50(64)	103.5(33)	-3.91(81)	7.1(18)	17.1(12)
C(15)	-0.43524(19)	0.13476(12)	0.24040(25)	64.9(18)	20.28(73)	75.9(30)	-9.99(92)	29.4(19)	13.4(12)
C(16)	-0.42595(17)	0.07318(12)	-0.32669(23)	45.5(16)	19.70(72)	57.7(27)	-9.93(86)	-0.2(16)	-5.4(11)
C)17)	-0.27759(17)	0.17557(12)	-0.29093(22)	47.5(15)	24.21(75)	45.0(26)	-9.84(86)	13.5(16)	4.2(11)
C(18)	-0.62418(16)	0.18664(12)	-0.11448(26)	27.8(13)	19.88(73)	105.8(33)	-4.97(79)	0.2(17)	6.4(12)
C()9)	-0.51537(17)	0.28892(12)	-0.18098(25)	43.3(15)	16.31(68)	83.3(30)	-1.85(81)	-10.0(17)	14.4(12)
C(21)	-0.18500(15)	0.40629(10)	0.48352(20)	28.2(12)	13.29(58)	36.3(22)	-1.58(67)	9.8(13)	2.02(91)
C(22)	-0.20075(15)	0.45706(10)	0.18155121)	34.5(13)	12.12(59)	45.0(23)	-2.47(70)	10.7(14)	5.92(94)
C(23)	-0.41044(15)	0.40716(11)	0.23428(21)	25.7(12)	12.73(59)	55.9(25)	0.04(68)	8.7(14)	0.94(96)
C(24)	-0.20240(17)	0.34288(11)	0.57570(22)	44.5(15)	18.35(68)	43.9(24)	0.55(80)	16.4(15)	8.9(10)
C(25)	-0.22051(16)	0.49182(11)	0.57103(22)	39.3(14)	15.21(64)	48.7(24)	-4.06(75)	11.5(15)	-3.7(10)
C(26)	-0.06765(17)	0.46514(11)	0.22293(23)	39.7(14)	16.47(66)	70.8(28)	-7.36(78)	13.9(16)	10.3(11)
C)27)	-0.24490(18)	0.44058(13)	-0.00302123)	54.2(17)	23.37(76)	49.7(26)	-7.15(90)	4.3(16)	15.6(11)
C(28)	-0.46843(16)	0.36905(12)	0.33796(24)	30.7(13)	19.67(71)	81.9(29)	-3.53(78)	22.3(16)	-0.1(11)
C(29)	-0.45224(17)	0.49747(12)	0.25029(24)	36.5(14)	17.04(69)	80.1(30)	5.92(79)	10.1(16)	5.4(11)
C(31)	0.07726(15)	0.18662(11)	0.05285(22)	27.3(13)	19.75(68)	48.6(24)	2.91(74)	13.3(14)	5.5(10)
C(32)	0.03322(16)	0.11805(10)	0.30922(22)	34.0(13)	11.40(58)	54.8(25)	1.82(70)	7.5(14)	5.64(97)
C(33)	0.11309(15)	0.28664(11)	0.37603(22)	26.5(13)	13.47(60)	56.8(25)	-3.36(69)	-1.0(14)	5.46(98)
C)34)	0.03572(17)	0.10939(12)	-0.06930(23)	43.7(15)	23.02(75)	53.5(26)	4.46(85)	16.6(16)	-4.3(11)
C(35)	0.05805(17)	0.25818(13)	-0.03220(23)	41.2(15)	27.74(82)	61.5(27)	0.38(88)	23.8(16)	17.3(12)
C(36)	-0.03663(18)	0.11974(12)	0.43992(24)	50.6(16)	16.06(67)	75.9(29)	-0.47(83)	19.4(17)	15.8(11)
C(37)	0.16205(17)	0.08486(12)	0.35921(25)	42.2(15)	18.40(71)	90.7(31)	6.85(83)	5.7(17)	14.3(12)
C(38)	0.24366(17)	0.27543(13)	0.36178(25)	29.3(14)	24.56(78)	86.2(31)	-7.88(83)	1.0(16)	7.2(12)
C(39)	0.10685(17)	0.29320(12)	0.55315(22)	37.9(14)	19.18(70)	48.3(25)	-1.35(80)	-1.9(15)	0.3(11)
H())	-0.1600(17)	0.1490(12)	0.0815(24)	1.68(39)					

[A] ESTIMATED STANDARD DEVIATIONS IN THE LEAST SIGNIFICANT FIGURE(S) ARE GIVEN IN PARENTHESES IN THIS AND ALL SUBSEQUENT TABLES. [B] THE FORM OF THE ANISOTROPIC THERMAL ELLIPSOID IS: $EXP(-(B11H^2+B22K^2+B33L^2+2B12HK+2B13HL+2B23KL))$. THE QUANTITIES GIVEN IN THE TABLE ARE THE THERMAL COEFFICIENTS X 10^4.

derived from a Patterson map, with the space group assumed to be the centrosymmetric group C_i^1-$P\bar{1}$. This choice is confirmed by the eventual successful refinement. All remaining nonhydrogen atoms were found in a subsequent Fourier map. After two cycles of isotropic refinement all the hydrogen atoms were easily found from a difference Fourier map, with peak heights in the range 0.60 (16) to 1.00 (16) e/Å^3. The alkyl hydrogen atoms were placed in idealized locations (C–H 0.95 Å, tetrahedral angles), each was given an isotropic thermal parameter B 1.0 Å^2 greater than that of its attached carbon atom, and all were held fixed during subsequent refinement. The hydrido hydrogen atom was initially given an isotropic thermal parameter B of 3.0 Å^2 and was refined isotropically in all remaining refinement cycles. The function $\sum w(F_o^2 - F_c^2)^2$ was minimized in the final cycle of least-squares refinement, which involved 284 variables and 8214 observations (including those for which $F_o^2 < 0$). This refinement converged to values of R and R_w (on F_o^2) of 0.041 and 0.061, respectively, to an error in an observation of unit weight of 1.15 electrons^2, and for those reflections having $F_o^2 > 3\sigma(F_o^2)$ to values of the conventional R and R_w indices on $|F_o|$ of 0.025 and 0.029, respectively. A listing of $10|F_o|$ vs. $10|F_c|$ and a table of alkyl hydrogen atom positions are available.[16] The final positional and thermal parameters of the nonhydrogen atoms and the hydrido hydrogen atom are listed in Table II. The final difference Fourier map has no peaks above 0.6 e/Å^3 except for two ripples (0.87 (9), 0.74 (9) e/Å^3) within 1 Å of the rhodium atom.

Results and Discussion

Syntheses and Spectra of Five- and Four-Coordinate Triethylphosphinehydridorhodium(I) Compounds. Recently we have reported that the reduction of mixtures of $RhCl_3$ and bulky tertiary phosphines with sodium amalgam in THF under a dinitrogen atmosphere yields a variety of Rh(I) hydrido compounds, e.g., *trans*-$RhH(N_2)L_2$ ($L = P(t\text{-}Bu)_3$, $PPh(t\text{-}Bu)_2$), $Rh_2H_2(\mu\text{-}N_2)L_4$ ($L = P(i\text{-}Pr)_3$, $P(c\text{-}C_6H_{11})_3$), and $RhHL_3$ ($L = P(i\text{-}Pr)_3$).[2,3,5] A similar reduction of $RhCl_3$ in the presence of excess PEt_3 gives the pentacoordinate complex $RhH(PEt_3)_4$ (**3**) as pale yellow crystals. This compound (**3**) is stable in the solid state below −20 °C under an argon atmosphere, but readily loses PEt_3 at room temperature. The isolation of a pure sample of compound **3** requires low-temperature manipulation and the presence of an excess of PEt_3; even with these precautions, carbon elemental analyses tend to give results lower than expected (see Experimental Section).

The ^1H NMR spectrum of **3** is temperature dependent. At −40 °C (toluene-d_8) the hydride signal is at δ −13.5 as a broad double quintet ($J_{H-Rh} = 8.0$, $J_{H-P} = 12.3$ Hz). As the temperature is raised the signal broadens and shifts to low field, δ −9.7 at 30 °C. At −35 °C the $^{31}P\{^1H\}$ NMR spectrum of **3** shows a sharp doublet at δ 11.4 ppm (see Experimental Section) ($J_{P-Rh} = 145.5$ Hz) together with signals assignable to **2** ($\delta \sim 26$ ppm, vide infra) and free PEt_3 (δ −23.8 ppm). The intensities of the latter signals were approximately 6 and 2%, respectively, of the major signal. The low-temperature $^{31}P\{^1H\}$ spectrum of a 1:2.5 mixture of **3** and PEt_3 shows only a sharp doublet at δ 10.9 ppm ($J_{P-Rh} = 145.5$ Hz) and a sharp singlet at δ −24.0 ppm, and resonances expected for **2** are absent. This suggests an equilibrium dissociation of PEt_3 from **3** (eq 1); the dissociation constant K_d has been determined spectroscopically (vide infra).

$$RhH(PEt_3)_4\ (\mathbf{3}) \overset{K_d}{\rightleftharpoons} RhH(PEt_3)_3\ (\mathbf{2}) + PEt_3 \qquad (1)$$

The A_4X pattern observed in the $^{31}P\{^1H\}$ NMR spectrum of **3** at −35 °C is consistent with a trigonal-bipyramidal structure rapidly undergoing a polytopal rearrangement, presumably via Berry pseudorotation. Such a facile rearrangement is well known for five-coordinate d^8 metal hydrido complexes, e.g., RhH(diphos)$_2$.[17] With continued cooling of the sample below −35 °C the spectrum continues to change (Figure 1). Below −50 °C signals of $RhH(PEt_3)_3$ and free PEt_3 disappear completely. The limiting spectrum is reached at −80 °C, and is an AB_3X pattern consisting of a doublet of doublets at δ 9.3 ppm ($J_{P_B-Rh} = 155$, $J_{P_B-P_A} = 37$ Hz) and a double quartet (δ 19.7 ppm, $J_{P_A-Rh} = 115$, $J_{P_A-P_B} = 37$ Hz). This limiting spectrum is consistent with a trigonal-bipyramidal structure, with the hydride ligand in an axial site. Good agreement of the magnitude of the observed value of the coupling constant J_{P-Rh} at −35 °C (145.5 Hz) with the weighted average computed from the limiting spectrum (145 Hz) indicates that the rapid exchange is intramolecular in the temperature range −35 to −80 °C. This is further confirmed by the observation that the temperature dependence of the $^{31}P\{^1H\}$ spectrum in this temperature range is unaffected by the presence of excess PEt_3.

The four-coordinate complex $RhH(PEt_3)_3$ (**2**) was readily obtained as a red oil in quantitative yield by the thermal decomposition of $RhH(PEt_3)_4$ (**3**) under vacuum at 60–65 °C (see

---

(16) See paragraph at end of paper regarding supplementary material.

(17) Jesson, J. P.; Muetterties, E. L. In "Dynamic Nuclear Magnetic Resonance Spectroscopy", Jackman, L. M., Cotton, F. A., Eds.; Academic Press: New York, 1975; pp 253-316.

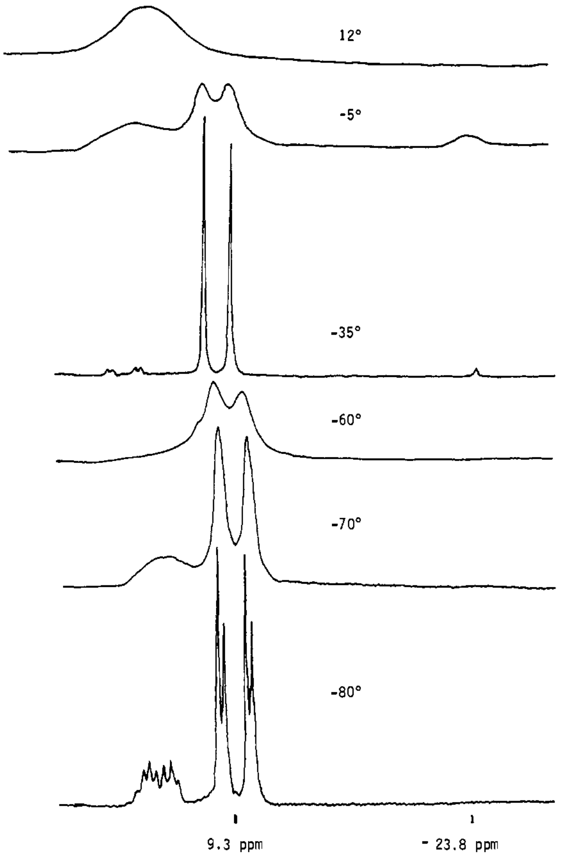

Figure 1. Variable temperature $^{31}P\{^1H\}$ NMR spectra of $RhH(PEt_3)_4$ (toluene-d_8). H_0 increases to the right.

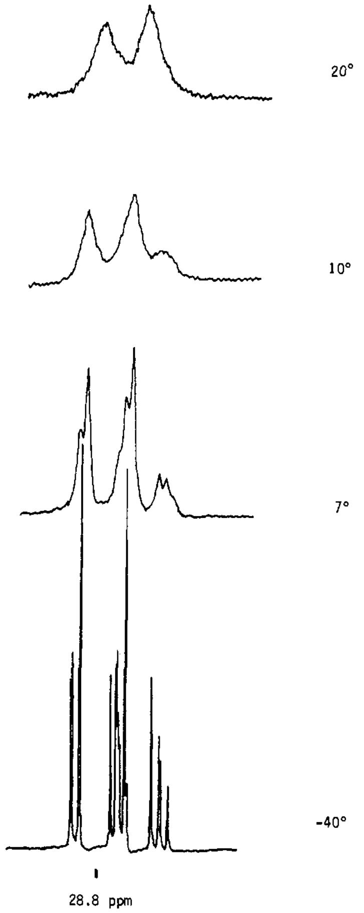

Figure 2. Variable temperature $^{31}P\{^1H\}$ NMR spectra of $RhH(PEt_3)_3$ (toluene-d_8). H_0 increases to the right.

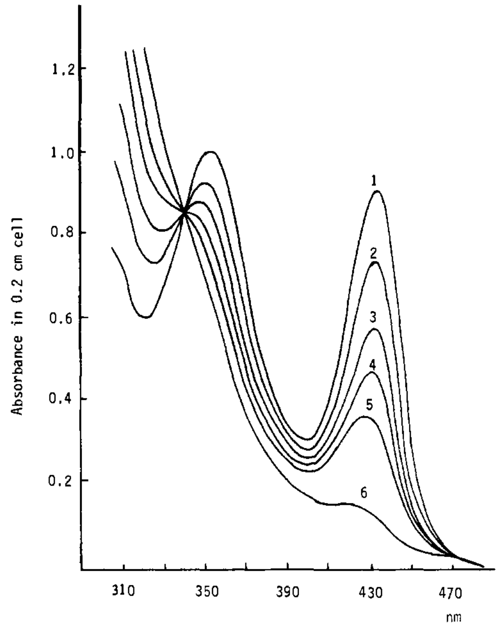

Figure 3. Electronic spectra of $RhH(PEt_3)_3$ (1.02×10^{-3} M) (*n*-heptane at 20 °C) with increasing concentration of added PEt_3: (1) none, (2) 0.027, (3) 0.068, (4) 0.136, (5) 0.271, (6) 1.080 M.

Table III. Preferred Numbers (*n*) of Coordinated Phosphine Ligands

	PEt_3	PPh_3	$P(i\text{-}Pr)_3$	$P(c\text{-}C_6H_{11})_3$	$P(t\text{-}Bu)_3$
$RhHL_n$	3,4	3,4	2,3	2	2
PtL_n	3,4	3,4	2,3	2	2

Experimental Section). At −50 °C (toluene-d_8) the hydrido NMR signal of **2** is a complex multiplet (AB_2MX spin system) centered at δ −7.90, which becomes a doublet (J_{H-Rh} = 18.0 Hz) when ^{31}P decoupled. As the temperature is raised the complex multiplet broadens and coalesces at 35 °C, owing to the intramolecular site exchange of the phosphine ligands (vide infra). The $^{31}P\{^1H\}$ NMR spectrum of **2** measured in toluene-d_8 at −40 °C is an AB_2X pattern (see Figure 2), fully consistent with a nominally square-planar structure. Nucleus P_A, the unique phosphorus atom (trans to H), gives rise to the low-field resonance (δ 28.8 ppm), and the higher-field resonances (centered at δ 25.4 ppm) are assigned to nuclei P_B. The decoupling constants are J_{P_A-Rh} = 137, J_{P_B-Rh} = 152, and $J_{P_A-P_B}$ = 28.5 Hz. As expected from the hydride NMR spectrum, the $^{31}P\{^1H\}$ NMR spectrum shows a reversible temperature dependence (Figure 2) with coalescence into a broad doublet occurring at 20 °C. The equilibration of the three phosphorus nuclei is taking place via an intramolecular process, since the coupling constant $J_{P_{av}-Rh}$ observed at 35 °C (146 Hz) is in excellent agreement with that calculated from the weighted average of J_{P_A-Rh} and J_{P_B-Rh} (calcd, 147 Hz). Line-shape analysis computations satisfactorily reproduce the observed temperature-dependent spectrum.

Observation of an isosbestic point in the electronic spectrum of $RhH(PEt_3)_3$ (**2**) with varying concentrations of added PEt_3 (Figure 3) confirms the equilibrium proposed in eq 1; the equilibrium constant for the dissociation (eq 1, K_d) is calculated to be 1.1×10^{-1} M (*n*-heptane, 20 °C). The spectrum of **2** itself, without added PEt_3, obeys Beer's law in the concentration range 1×10^{-2} to 5×10^{-4} M and this suggests to us that further loss of PEt_3 from **2** to give $RhH(PEt_3)_2$ is negligibly small.

Facile dissociation of PEt_3 from the present d^8 system, $RhH(PEt_3)_4$ (**3**), is analogous to the PEt_3 dissociation from the nominally isoelectronic d^{10} system $Pt(PEt_3)_4$[18] ($K_d = 3.0 \times 10^{-1}$ M in *n*-heptane at 20 °C). In fact there is a remarkable parallel

---

[18] Yoshida, T.; Matsuda, T.; Okano, T.; Kitani, T.; Otsuka, S. *J. Am. Chem. Soc.* **1979**, *101*, 2027–2038.

Table IV. Selected Bond Distances (Å) and Angles (deg) in $RhH(P(i\text{-}Pr)_3)_3$

Rh-P(1)	2.291(1)	P(1)-Rh-P(2)	109.15 (3)
Rh-P(2)	2.330(1)	P(1)-Rh-P(3)	141.52(3)
Rh-P(3)	2.297(1)	P(1)-Rh-H(1)	71.7(7)
Rh-H(1)	1.58(2)	P(2)-Rh-P(3)	109.32(3)
P(1)-C(11)	1.868(2)	P(2)-Rh-H(1)	177.2(7)
P(1)-C(12)	1.870(2)	P(3)-Rh-H(1)	69.9 (7)
P(1)-C(13)	1.880(2)	C(11)-P(1)-Rh	112.24(6)
P(2)-C(21)	1.869(2)	C(12)-P(1)-Rh	109.28(6)
P(2)-C(22)	1.866(2)	C(13)-P(1)-Rh	125.28(6)
P(2)-C(23)	1.876(2)	C(21)-P(2)-Rh	113.76(6)
P(3)-C(31)	1.870(2)	C(22)-P(2)-Rh	117.92(7)
P(3)-C(32)	1.870(2)	C(23)-P(2)-Rh	116.66(6)
P(3)-C(33)	1.894(3)	C(31)-P(3)-Rh	110.52(7)
P-C (av)[a]	1.874(9)	C(32)-P(3)-Rh	109.39(6)
C(11)-C(14)	1.527(3)	C(33)-P(3)-Rh	126.38(6)
C(11)-C(15)	1.532(2)	C(11)-P(1)-C(12)	101.79(9)
C(12)-C(16)	1.527(3)	C(11)-P(1)-C(13)	99.99(8)
C(12)-C(17)	1.531(3)	C(12)-P(1)-C(13)	105.58(9)
C(13)-C(18)	1.536(3)	C(21)-P(2)-C(22)	102.05(8)
C(13)-C(19)	1.535(3)	C(21)-P(2)-C(23)	105.55(8)
C(21)-C(24)	1.538(3)	C(22)-P(2)-C(23)	98.75(8)
C(21)-C(25)	1.529(2)	C(31)-P(3)-C(32)	101.96(9)
C(22)-C(26)	1.519(3)	C(31)-P(3)-C(33)	100.13(9)
C(22)-C(27)	1.533(3)	C(32)-P(3)-C(33)	105.65(9)
C(23)-C(28)	1.530(3)	C(14)-C(11)-C(15)	109.7(2)
C(23)-C(29)	1.534(3)	C(16)-C(12)-C(17)	110.5(2)
C(31)-C(34)	1.530(3)	C(18)-C(13)-C(19)	109.4(2)
C(31)-C(35)	1.530(3)	C(24)-C(21)-C(25)	110.3(2)
C(32)-C(36)	1.535(3)	C(26)-C(22)-C(27)	109.3(2)
C(32)-C(37)	1.532(3)	C(28)-C(23)-C(29)	109.9(2)
C(33)-C(38)	1.536(3)	C(34)-C(31)-C(35)	110.0(2)
C(33)-C(39)	1.534(3)	C(36)-C(32)-C(37)	111.1(2)
C-C (av)	1.532(4)	C(38)-C(33)-C(39)	109.2(2)

[a] The value in parentheses for an average value is the standard deviation of a single observation and is the larger of that estimated from the average standard deviation of the individual observations or on the assumption that the values averaged are from the same population.

in the trends for the preferred numbers of coordinated phosphine ligands (n) between the systems PtL_n[19] and $RhHL_n$,[5] as summarized in Table III.

Description of the Structure. Figure 4 is a drawing of compound **1**, $RhH(P(i\text{-}Pr)_3)_3$. The complex is almost perfectly planar. The average deviation of the phosphorus and rhodium atoms from the best weighted least-squares plane is 0.006 Å. The hydrido ligand is computed to be 0.08 (2) Å from this plane. Angles around the rhodium atom (see Table IV) are badly distorted from ideal "square planar." The angle P(1)-Rh-P(3) between the nominally trans phosphine ligands is 141.52 (3)°. The average H-Rh-P(cis) angle is 70.7 (14)° and is the smallest reported for a planar four-coordinate complex (vide infra). This is the result of the unusual amount of steric crowding among the three triisopropylphosphine ligands, although nominally trans phosphine ligands have a tendency to bend toward a mutually cis hydrido ligand even in the absence of such extreme steric crowding.[2,5,20] The Rh-P(1) and Rh-P(3) bond distances (see Table IV) are essentially equal (av 2.294 (4) Å) and are significantly shorter than the Rh-P(2) bond distance (2.330 (1) Å), which is lengthened as a result of the large trans influence of the hydrido ligand.[11] The Rh-H bond distance (1.58 (2) Å) is normal.

Some sizable distortions exist within the triisopropylphosphine ligands. In each of the two mutually trans phosphine ligands there is a C-P-Rh angle considerably greater than 125°. More typical C-P-Rh angles in less crowded $P(i\text{-}Pr)_3$ complexes are 111-117°[4,5,7,21] (Table V). This large angle in the present complex reflects the extreme steric crowding imposed upon the molecule by the presence of three rather bulky triisopropylphosphine ligands (nominal cone angle 160°;[22] see also ref 23). The angles C-P-C are only slightly different from normal values in other $P(i\text{-}Pr)_3$ complexes. It appears as though the two mutually trans phosphine ligands have accommodated their neighboring cis phosphine not only by bending toward the hydrido ligand, permitted by its relatively small steric requirements, but also by bending the rhodium-phosphorus bond, illustrated below in I. The dashed lines in I represent the pseudo-C_3 axis of the PR_3 ligands, which is also the direction of maximum electron density in the sp^3-hybridized lone pairs; in an undistorted complex the dashed lines would lie along, or within ca. 3° of, the P-Rh interatomic vectors. In this present complex we estimate the angle ϕ (see I) between the sp^3 hybrid and the P-Rh vector to be 12°.

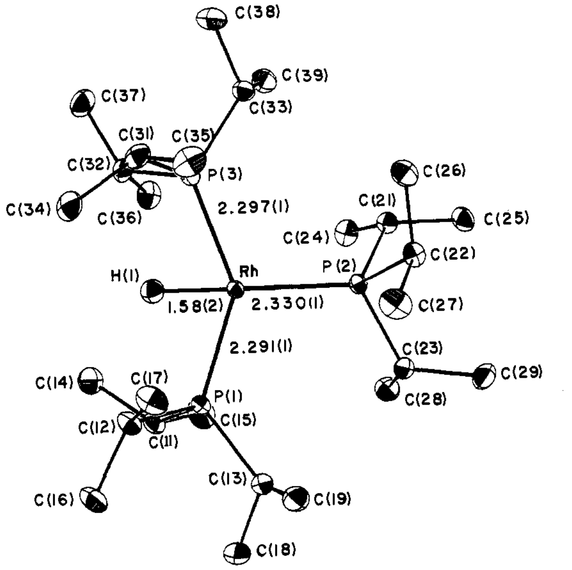

Figure 4. A drawing of a molecule of $RhH(P(i\text{-}Pr)_3)_3$. Thermal ellipsoids are drawn at the 50% probability level here and in Figure 5. Selected interatomic distances are given. Alkyl hydrogen atoms have been omitted.

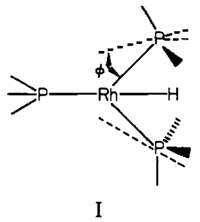

I

The X-ray structures of two other tris(phosphine)hydrido d^8 metal complexes, $RhH(PPh_3)_3$[11] and $PtH(PPh_3)_3{}^+$,[24] have been reported. Both of these complexes have a planar structure similar to that of the present complex, but with angles around the metal less distorted from "square planar": the P-metal-P(trans) angles are 151.7 (2)° in $RhH(PPh_3)_3$ and 159.6 (2)° in $PtH(PPh_3)_3{}^+$ (compare 141.52 (3)° in the present structure). This is the expected consequence of the larger steric bulk of the triisopropylphosphine ligands.

The crystal packing is shown in Figure 5. It appears to be determined by intermolecular van der Waals' and steric interactions among the alkyl hydrogen atoms. The closest intermolecular H···H contact is 2.37 Å (H(1)C(27)-H(3)C(29)). The shortest Rh···H(alkyl) distance is 3.02 Å (Rh-H(2)C(36)).

The Rearrangement Process in $RhHL_3$ Compounds (1, L = $P(i\text{-}Pr)_3$; 2, L = PEt_3). Rapid intramolecular rearrangement in nominally square-planar $RhXL_3$ complexes has been elegantly

---

(19) Otsuka, S.; Yoshida, T.; Matsumoto, M.; Nakatsu, K. *J. Am. Chem. Soc.* **1976**, *98*, 5850-5858.

(20) Frenz, B. A.; Ibers, J. A. In "Transition Metal Hydrides", Muetterties, E. L., Ed.; Marcel Dekker: New York, 1971; Chapter 3.

(21) Busetto, C.; D'Alfonso, A.; Maspero, F.; Perego, G.; Zazzetta, A. *J. Chem. Soc., Dalton Trans.* **1977**, 1828-1834.

(22) Tolman, C. A. *Chem. Rev.* **1977**, *77*, 313-348.

(23) Immirzi, S.; Musco, A. *Inorg. Chim. Acta* **1977**, *25*, L41-L42.

(24) Caputo, R. E.; Mak, D. K.; Willett, R. D.; Roundhill, S. G. N.; Roundhill, D. M. *Acta Crystallogr., Sect. B* **1977**, *33*, 215-218.

Table V. Comparison of Rh-P-C and C-P-C Angles with Other $RhP(i\text{-}Pr)_3$ Structures

angle	structure: $RhCl(N_2)(P(i\text{-}Pr)_3)_2$[a]	$RhCl(X)(P(i\text{-}Pr)_3)_2$[b]	$[RhH(P(i\text{-}Pr)_3)_2]_2(\mu\text{-}N_2)$[c]	$RhH(P(i\text{-}Pr)_3)_3$[d]	$RhH_2(O_2COH)(P(i\text{-}Pr)_3)_2$[e]
Rh-P-C	111.26(5) to 113.43(5)[f]	110.5(2) to 116.4(1)	112.5(2) to 114.0(2)	109.28(6) to 126.38(6)	109.93(7) to 117.33(10)
C-P-C	103.89(7) to 110.17(7)	102.4(1) to 110.3(2)	102.9(3) to 109.7(3)	98.75(8) to 105.65(9)	101.75(12) to 105.81(11)

[a] Reference 7. [b] $X = N_2, C_2H_4$, ref 21. [c] Reference 5. [d] Present work. [e] Reference 4. [f] The two numbers listed are the smallest and largest of the Rh-P-C angles published for this structure. The numbers in parentheses are the estimated standard deviations for those angles.

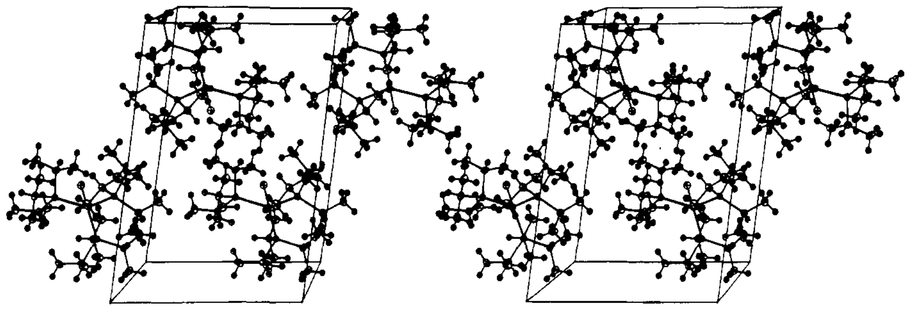

Figure 5. Stereoscopic view of the unit cell contents of $RhH(P(i\text{-}Pr)_3)_3$. Alkyl hydrogen atoms are included with an artificial isotropic B of 1.0 Å^2. The crystallographic a axis runs from left to right and the b axis from bottom to top. The point (0,0,0) is at the center of each drawing.

established for $RhH(PPh_3)_3$,[11] and has been suggested for $Rh(CH_3)(PPh_3)_3$[11,25] and $Rh(C_6H_5)(PMe_3)_3$.[26] The complex $NiH(PEt_3)_3{}^+$[27] also appears to undergo such a rearrangement. Site exchange among the phosphine ligands of **1**, $RhH(P(i\text{-}Pr)_3)_3$, is more facile than in both $RhH(PEt_3)_3$ (**2**) and $RhH(PPh_3)_3$. The $^{31}P\{^1H\}$ NMR spectrum of **1** consists of a sharp doublet throughout the temperature range −51 to +36 °C (δ 32.2 ppm; $J_{P\text{-}Rh} = 157$ Hz at −51 °C, 156.5 Hz at +36 °C), consistent with an intramolecular process. In the series of square-planar $RhHL_3$ complexes the coalescence temperature increases in the order $P(i\text{-}Pr)_3$ (<−50 °C) < PPh_3 (−13 °C)[11] < PEt_3 (20 °C). The order is inexplicable in terms of the electronic properties of the phosphine ligands, but correlates well with their steric bulk (cone angle:[22] PEt_3, 132°; PPh_3, 145°; $P(i\text{-}Pr)_3$, 160°). We had initially expected that $RhH(P(i\text{-}Pr)_3)_3$ would have a geometry considerably distorted from planarity, possibly toward a pseudotetrahedral geometry which is the suggested transition state for the intramolecular rearrangement process.[11] Unexpectedly $RhH(P(i\text{-}Pr)_3)_3$ exhibits an essentially perfectly planar structure.

If the intramolecular ligand site exchange occurs through a planar $\rightleftharpoons$ pseudotetrahedral process, the latter should be the transition state.[28] What we observe in the static form of $RhH(P(i\text{-}Pr)_3)_3$ is a perfectly planar structure with a large P(1)–Rh–P(2) angle (109°). The observed angles around the phosphorus atoms imply that considerable steric strain is involved in the planar molecule. This strain would not be relieved by rearrangement into a tetrahedral geometry, since the P_A–Rh–P_B angle would remain nearly the same (ca. 110°). We therefore propose the following alternative mechanism (II). This mechanism differs

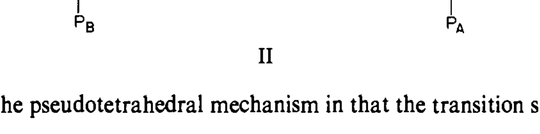

II

from the pseudotetrahedral mechanism in that the transition state is more properly described as having a trigonal-pyramidal geometry with P–Rh–P angles approaching 120°.[29] A process in which the hydrido ligand moves above (or below) the coordination plane is ordinarily thought to be endoenergetic in "square-planar" complexes, but some of the required energy can be obtained by relief of steric strain among the triisopropylphosphine ligands. The strain would be very small in the planar PEt_3 complex, explaining the relative stereochemical stability. It must, however, be noted that, if the H–Rh–P angle in the trigonal-pyramidal transition state[28] becomes larger than 90°, the structure approaches a pseudotetrahedron. Since the permutational set is the same for either transition-state geometry, it is impossible to distinguish experimentally between the two routes of polytopal rearrangement.[27,30] Both routes resemble the "tetrahedral jump" mechanism proposed for the rearrangement of $MH(PX_3)_4$ molecules.[27,31]

Planar $RhCl(PPh_3)_3$ is known to be stereochemically rigid.[32] Strictly on the basis of steric effects, the pseudotetrahedral transition state should be reached more readily by $RhCl(PPh_3)_3$ than by $RhH(PPh_3)_3$ because of the larger size of Cl^- compared with H^-. This is contrary to what is observed and is perhaps indicative of the special electronic nature of the hydrido ligand.

Formation of the Complex. It is not obvious how single crystals of compound **1**, $RhH(P(i\text{-}Pr)_3)_3$, could have been formed from a reaction solution originally containing only $[RhH(P(i\text{-}Pr)_3)_2]_2(\mu\text{-}N_2)$. The procedure is repeatable. We suspect that the initial reaction in solution is a dissociation of the dinitrogen-bridged dimer (eq 2), followed by loss of N_2 from the resulting monomer (eq 3),[4,5] assisted by the argon purge. The partial decomposition of $RhH(P(i\text{-}Pr)_3)_2$ (eq 4) results in the release of free phosphine molecules which are scavenged by remaining $RhH(P(i\text{-}Pr)_3)_2$ to form $RhH(P(i\text{-}Pr)_3)_3$ (eq 5).

$$[RhH(P(i\text{-}Pr)_3)_2]_2(\mu\text{-}N_2) \rightarrow RhH(P(i\text{-}Pr)_3)_2 + RhH(N_2)(P(i\text{-}Pr)_3)_2 \quad (2)$$

$$RhH(N_2)(P(i\text{-}Pr)_3)_2 \rightleftharpoons N_2 + RhH(P(i\text{-}Pr)_3)_2 \quad (3)$$

$$RhH(P(i\text{-}Pr)_3)_2 \xrightarrow[\text{dec}]{} ? + P(i\text{-}Pr)_3 \quad (4)$$

$$RhH(P(i\text{-}Pr)_3)_2 + P(i\text{-}Pr)_3 \rightarrow RhH(P(i\text{-}Pr)_3)_3 \quad (5)$$

---

(25) Keim, W. *J. Organomet. Chem.* **1967**, *8*, P25–P26. Dewhirst, K. C.; Keim, W.; Reilly, C. A. *Inorg. Chem.* **1968**, *7*, 546–551.

(26) Jones, R. A.; Wilkinson, G. *J. Chem. Soc., Dalton Trans.* **1979**, 472–477.

(27) English, A. D.; Meakin, P.; Jesson, J. P. *J. Am. Chem. Soc.* **1976**, *98*, 422–436.

(28) Strictly speaking, the transition state cannot have C_3 or C_{3v} symmetry: Stanton, R. E.; McIver, J. W., Jr. *J. Am. Chem. Soc.* **1975**, *97*, 3622–3646. However, the true transition state need be only minutely distorted from C_3 symmetry to satisfy the requirements deduced by these authors.

(29) Extended Hückel calculations suggest that such a structure could be diamagnetic (low spin): Strauss, S. H., personal communication; Ph.D. Thesis, Northwestern University, 1979.

(30) Jesson, J. P.; Meakin, P. *Acc. Chem. Res.* **1973**, *6*, 269–275.

(31) Meakin, P.; Jesson, J. P.; Tebbe, F. N.; Muetterties, E. L. *J. Am. Chem. Soc.* **1971**, *93*, 1797–1799.

(32) Tolman, C. A.; Meakin, P. Z.; Lindner, D. L.; Jesson, J. P. *J. Am. Chem. Soc.* **1974**, *96*, 2762–2774.

The nature of reaction 4 is not presently known. Decomposition of $RhH(P(i\text{-}Pr)_3)_2$ may be indicative of the formation of as-yet-uncharacterized clusters. The orange, plate-like crystals which also grew in the reaction solution (see Experimental Section) may contain the elusive complex $[RhH(P(i\text{-}Pr)_3)_2]_2$[5] but none of these crystals diffracts X-rays, and the true nature of the remaining compound(s) is presently unknown.

Acknowledgment. We are indebted to Johnson Matthey, Inc., Malvern, Pa., for the loan of Rh metal used in this work. This work was kindly supported by the National Science Foundation (CHE76-10335) and the Japanese Society for the Promotion of Science. Support is also acknowledged from the Japan-U.S. Cooperative Science Program (GR021/INT 77-07152). We also wish to thank Dr. P. J. Domaille of E. I. du Pont de Nemours and Co. for valuable assistance with the line shape analysis calculations.

Supplementary Material Available: A listing of observed and calculated structure amplitudes and a table of alkyl hydrogen atom positions (29 pages). Ordering information is given on any current masthead page.

Mechanism of Thermal Decomposition of *trans*-Diethylbis(tertiary phosphine)palladium(II). Steric Effects of Tertiary Phosphine Ligands on the Stability of Diethylpalladium Complexes

Fumiyuki Ozawa, Takashi Ito, and Akio Yamamoto*[1]

Contribution from the Research Laboratory of Resources Utilization, Tokyo Institute of Technology, Nagatsuta, Midori-ku, Yokohama 227, Japan. Received March 27, 1980

Abstract: *trans*-$[PdR'_2(PR_3)_2]$ with a series of alkyl groups and tertiary phosphine ligands of various steric bulkiness (R' = Et, PR_3 = PMe_2Ph (**1**), PEt_3 (**2**), PEt_2Ph (**3**), $PMePh_2$ (**4**), $PEtPh_2$ (**5**); R' = Pr (**6**), Bu (**7**), PR_3 = PMe_2Ph) are thermolyzed in solution by β-elimination processes liberating alkane and alkene in a 1:1 ratio. Kinetic studies on thermolysis of *trans*-$[PdEt_2(PR_3)_2]$ revealed that they decompose obeying the first-order rate law with respect to the concentration of the palladium complexes. Thermolysis predominantly proceeds from the four-coordinated complex without dissociation of the tertiary phosphine ligand. The minor parallel thermolysis pathway involving the dissociation of the phosphine is completely blocked by addition of the phosphine. Activation enthalpies for thermolysis of the ethylpalladium complexes having various steric bulkiness were virtually constant in the range of 26.0 ± 1.0 kcal/mol whereas activation entropies showed considerable variation with increasing bulkiness of the phosphine. Thermolysis of *trans*-$[Pd(CH_2CD_3)_2(PMePh_2)_2]$ (**8**) cleanly liberated $CH_2{=}CD_2$ and CH_2DCD_3 with a small isotope effect ($k_H/k_D = 1.4 \pm 0.1$). The kinetic results together with examination of the molecular model suggest that the interaction between the bulky phosphine ligands and the ethyl groups causes the destabilization of the Pd-Et bonds. A thermolysis mechanism consistent with the kinetic results assuming an activation state distorted from the square-planar ground state is proposed.

Introduction

Tertiary phosphines are employed in a variety of transition-metal-promoted reactions to control the reaction courses.[2] Understanding of their influence on the stability and reactivity of organometallic species involved in these reactions is expected to provide essential information in clarifying the reaction mechanisms and further designing suitable catalytic reactions promoted by transition-metal catalysts. Effectiveness of tertiary phosphines as auxiliary stabilizing ligands of transition-metal alkyls is well-known as exemplified by an increasing number of successful isolations of transition-metal alkyls having tertiary phosphine ligands.[2e] Although some proposals have been made for accounting for the stability of transition-metal alkyls,[3] the exact reason for the stabilization effect of the tertiary phosphine ligands is still far from clear. The role of tertiary phosphine ligands in stabilizing transition-metal alkyls may be accounted for in terms of electronic and steric factors. An attempt to interpret the stabilization effect of tertiary phosphines and related ligands in terms of the electronic effect as the increase in the ligand field energy to cause the electronic excitation of transition-metal alkyls has been made by Chatt and Shaw,[4] whereas Wilkinson pointed out the importance of the role of auxiliary ligands as a blocking agent to hinder the occurrence of β elimination as the most frequently observed decomposition pathway.[5] There are some examples that show the dissociation of tertiary phosphines is quite important in initiating the thermolysis of transition-metal alkyls,[6] but other examples indicate that explanation of the role of the auxiliary ligands in transition-metal alkyls merely as the blocking agent for the β-elimination process is insufficient.[7] For getting more information concerning the role of the stabilizing ligands on transition-metal alkyls, we have undertaken the kinetic study of thermolysis of

---

[1] Author to whom correspondence should be addressed.

[2] For example: (a) Tsuji, J. "Organic Synthesis by Means of Transition Metal Complexes"; Springer-Verlag: Berlin and Heidelberg, 1975. (b) Heck, R. F. "Organotransition Metal Chemistry"; Academic Press: New York, 1974. (c) Green, M. L. H. "Organometallic Compounds, Vol. 2; The Transition Elements"; Methuen: London, 1968. (d) Bird, C. W. "Transition Metal Intermediates in Organic Synthesis"; Academic Press: London, 1967. (e) McAuliffe C. A.; Levason, W. "Phosphine, Arsine and Stibine Complexes of the Transition Elements"; Elsevier: Amsterdam, Oxford, and New York, 1979.

[3] (a) Kochi, J. K. "Organometallic Mechanisms and Catalysis"; Academic Press: New York, 1978. (b) Davidson, P. J.; Lappert, M. F.; Pearce, R. *Chem. Rev.* **1976**, *76*, 219. (c) Schrock, R. R.; Parshall, G. W. *Ibid.* **1976**, *76*, 243. (d) Taube, R.; Drevs, H.; Steinborn, D. *Z. Chem.* **1978**, *18*, 425.

[4] (a) Chatt, J.; Shaw, B. L. *J. Chem. Soc.* **1959**, 705. (b) Chatt, J.; Shaw, B. L. *Ibid.* **1960**, 1718.

[5] Mowat, W.; Yagupsky, S. G.; Hill, N. J.; Yagupsky, M.; Wilkinson, G. *J. Chem. Soc., Dalton Trans.* **1972**, 533.

[6] (a) Whitesides, G. M.; Gaasch, J. F.; Stedronsky, E. R. *J. Am. Chem. Soc.* **1972**, *94*, 5258. (b) Reger, D. L.; Culbertson, E. C. *Ibid.* **1976**, *98*, 2789.

[7] Yamamoto, A.; Yamamoto, T., submitted for publication in *Acc. Chem. Res.*

0002-7863/80/1502-6457$01.00/0 © 1980 American Chemical Society